Convergent Evolution of Endosymbiont Differentiation in Dalbergioid and Inverted Repeat-Lacking Clade Legumes Mediated by Nodule-Specific Cysteine-Rich Peptides[1]

Pierre Czernic[2], Djamel Gully[2], Fabienne Cartieaux, Lionel Moulin, Ibtissem Guefrachi, Delphine Patrel, Olivier Pierre, Joël Fardoux, Clémence Chaintreuil, Phuong Nguyen, Frédéric Gressent, Corinne Da Silva, Julie Poulain, Patrick Wincker, Valérie Rofidal, Sonia Hem, Quentin Barrière, Jean-François Arrighi, Peter Mergaert, and Eric Giraud*

Université de Montpellier, F–34095 Montpellier cedex 5, France (P.C.); Institut de Recherche pour le Développement, Laboratoire des Symbioses Tropicales et Méditerranéennes, Unité Mixte de Recherche Institut de Recherche pour le Développement/SupAgro/Institut National de la Recherche Agronomique/Université de Montpellier/Centre de Coopération Internationale en Recherche Agronomique pour le Développement, Campus International de Baillarguet, 34398 Montpellier cedex 5, France (D.G., F.C., L.M., D.P., J.F., C.C., P.N., F.G., J.-F.A., E.G.); Institute for Integrative Biology of the Cell, Unité Mixte de Recherche 9198, Centre National de la Recherche Scientifique/Université Paris-Sud/Commissariat à l'Energie Atomique, 91198 Gif-sur-Yvette, France (I.G., O.P., Q.B., P.M.); Commissariat à l'Energie Atomique, Direction des Sciences du Vivant, Institut de Génomique, Génoscope, 91000 Evry, France (C.D.S., J.P., P.W.); and Laboratoire de Protéomique Fonctionnelle, Institut National de la Recherche Agronomique, Unité de Recherche 1199, 34060 Montpellier, France (V.R., S.H.)

ORCID IDs: 0000-0003-2845-6192 (P.C.); 0000-0002-4439-3454 (C.C.); 0000-0001-9614-4508 (P.N.); 0000-0002-5919-7317 (P.M.); 0000-0002-4190-1732 (E.G.).

Nutritional symbiotic interactions require the housing of large numbers of microbial symbionts, which produce essential compounds for the growth of the host. In the legume-rhizobium nitrogen-fixing symbiosis, thousands of rhizobium microsymbionts, called bacteroids, are confined intracellularly within highly specialized symbiotic host cells. In Inverted Repeat-Lacking Clade (IRLC) legumes such as *Medicago* spp., the bacteroids are kept under control by an arsenal of nodule-specific cysteine-rich (NCR) peptides, which induce the bacteria in an irreversible, strongly elongated, and polyploid state. Here, we show that in *Aeschynomene* spp. legumes belonging to the more ancient Dalbergioid lineage, bacteroids are elongated or spherical depending on the *Aeschynomene* spp. and that these bacteroids are terminally differentiated and polyploid, similar to bacteroids in IRLC legumes. Transcriptome, in situ hybridization, and proteome analyses demonstrated that the symbiotic cells in the *Aeschynomene* spp. nodules produce a large diversity of NCR-like peptides, which are transported to the bacteroids. Blocking NCR transport by RNA interference-mediated inactivation of the secretory pathway inhibits bacteroid differentiation. Together, our results support the view that bacteroid differentiation in the Dalbergioid clade, which likely evolved independently from the bacteroid differentiation in the IRLC clade, is based on very similar mechanisms used by IRLC legumes.

Legumes, thanks to their ability to develop a symbiotic interaction with nitrogen-fixing bacteria, collectively called rhizobia, are among the agronomically and ecologically most important plants. This symbiosis results in the formation of new organs, the nodules, inside which rhizobia differentiate into an endosymbiotic form, the bacteroids, able to fix atmospheric nitrogen to the benefit of the plant. During this differentiation step, profound modifications of the metabolism of the rhizobia are observed, and this can be accompanied by a marked change in the bacterial cell shape and size (Haag et al., 2013). Three distinct bacteroid morphotypes have been observed in different legume species (Oono et al., 2010; Bonaldi et al., 2011; Kondorosi et al., 2013; Supplemental Fig. S1A): (1) elongated or E-morphotype bacteroids described in legumes of the Inverted Repeat-Lacking Clade (IRLC; *Medicago*, *Pisum*, and *Vicia* spp.) and some *Aeschynomene* spp. such as *Aeschynomene afraspera*; (2) enlarged, spherical

bacteroids (S-morphotype) encountered in some species of the Dalbergioid clade (such as *Aeschynomene indica*, *Aeschynomene evenia*, and *Arachis hypogaea*); and (3) unmodified bacteroids (U-morphotype), which display a rod-shape morphology similar to free-living bacteria found in phaseoloid or robinoid legumes (i.e. *Phaseolus*, *Vigna*, *Lotus*, *Glycine*, and *Sesbania* spp.). The fact that the same rhizobium strain nodulating legumes of different clades can display different morphotypes is strong evidence supporting the conclusion that the host plant governs the bacteroid morphotype (Sen and Weaver, 1984; Mergaert et al., 2006; Bonaldi et al., 2011). The change of shape is probably the tip of the iceberg of the control exerted by the plant on the bacteria physiology during symbiosis. Indeed, besides their E-morphotype, the *Sinorhizobium meliloti* bacteroids in *Medicago truncatula* differ from their free-living state in several respects: they become polyploid, their membrane permeability increases dramatically, and they lose their reproductive capacity. Bacteroids that display such extreme changes are considered as terminally differentiated because they are unable to revert to their bacterial form (Mergaert et al., 2006).

In *M. truncatula*, a class of peptides, named nodule-specific cysteine-rich (NCR) peptides, plays a key role in this terminal bacteroid differentiation (Van de Velde et al., 2010). The *M. truncatula* NCR family is composed of about 600 highly divergent genes, which are nearly all expressed exclusively in nodules (Mergaert et al., 2003; Alunni et al., 2007; Young et al., 2011). NCR peptides are similar to the defensin type of antimicrobial peptides. The peptides contain an N-terminal secretion signal, and the mature peptides are usually no longer than 60 amino acids and have four to six conserved Cys residues (Mergaert et al., 2003). The cleavage of the signal peptide by a nodule-specific signal peptidase complex (SPC) located in the endoplasmic reticulum is required to permit the trafficking of NCR peptides to the symbiosome compartment. Bacteroid and symbiosome development is blocked in *M. truncatula defective in nitrogen fixation1* (*dnf1*) mutant that is affected in the SPC22 subunit of this nodule-specific SPC (Van de Velde et al., 2010; Wang et al., 2010). Some NCR peptides have been found to have antimicrobial activity, killing rhizobium when applied at high concentrations (Van de Velde et al., 2010). However, these antimicrobial peptide-like NCR peptides can, at lower concentrations, induce typical features of E-morphotype bacteroids in vitro on cultured rhizobia (Van de Velde et al., 2010). The NCR gene family has been identified in all investigated legume species of the IRLC clade but in no other plant species outside of this clade. This raises the question about the nature of the factors used by the other legumes to control bacteroid metamorphosis.

In the Dalbergioid legume clade, bacteroids can be of the E- or S-morphotype. For example, within the *Aeschynomene* genus, *A. afraspera* has E-type bacteroids but *A. indica* or *A. evenia* have S-type bacteroids (Bonaldi et al., 2011; Arrighi et al., 2012). The bacteroid morphogenesis in the *Aeschynomene* genus is also under plant

control, since the *Bradyrhizobium* spp. strain ORS285 transforms into E-morphotype bacteroids in *A. afraspera* nodules and in S-morphotype bacteroids in *A. indica* and *A. evenia* nodules (Bonaldi et al., 2011; Arrighi et al., 2012). The *Aeschynomene* symbiosis with *Bradyrhizobium* spp. has several other particular features, including the formation of nodules on both roots and stems, photosynthesis by the *Bradyrhizobium* symbionts that is required for optimal stem nodulation (Giraud et al., 2000), and the use of a Nod factor-independent nodulation pathway in some *Aeschynomene* spp., including *A. indica* and *A. evenia* (Giraud et al., 2007; Arrighi et al., 2012). Furthermore, in contrast to classical determinate and indeterminate nodules, aeschynomenoid nodules originate from the successive divisions of only one or a few root cortical cells initially infected by an infection thread-independent mechanism (Bonaldi et al., 2011). This infection mechanism has two consequences: (1) all the nodule primordium cells are infected, and (2) all the nodule primordium cells and bacteria are synchronized. Thus, during the nodule development of *A. indica* nodules, the differentiation of bacteroids occurs simultaneously for all nodule cells and takes place between days 4 and 5 after inoculation (Bonaldi et al., 2011). The possibility for obtaining samples of homogenous material at different differentiation stages and the existence of two distinct bacteroid morphotypes in closely related species make the *Bradyrhizobium-Aeschynomene* symbiotic couples an appealing model system for unraveling the mechanisms of bacteroid morphotype determination in legume species outside the IRLC clade.

In this study, we show that E- and S-morphotype bacteroids from *A. afraspera* and *A. indica* nodules display typical features of terminal differentiation. Furthermore, in these two species, we reveal the presence of an NCR-like peptide family that is specifically produced in the nodules and targets the bacteroids. Alteration of the trafficking of these peptides by silencing the *dnf1* homolog identified in *A. evenia* correlated with the absence of bacterial differentiation, indicating that the NCR-like peptides identified in *Aeschynomene* spp. play a similar role to those described in *Medicago* spp.. Altogether, these data support the hypothesis of a convergent evolution of the host molecular mechanisms governing bacteroid differentiation in legumes.

RESULTS

E- and S-Bacteroids in *Aeschynomene* spp. Are Terminally Differentiated

Previous studies revealed that *Bradyrhizobium* sp. strain ORS285 displayed two distinct bacteroid morphotypes according to the *Aeschynomene* spp. host: E-morphotype in *A. afraspera* and S-morphotype in *A. indica* (Fig. 1A; Bonaldi et al., 2011). As this difference in shape could imply different properties, we analyzed in each bacteroid type, isolated from mature nodules at 14 d post inoculation (dpi), several characteristics that have been shown to change during bacteroid
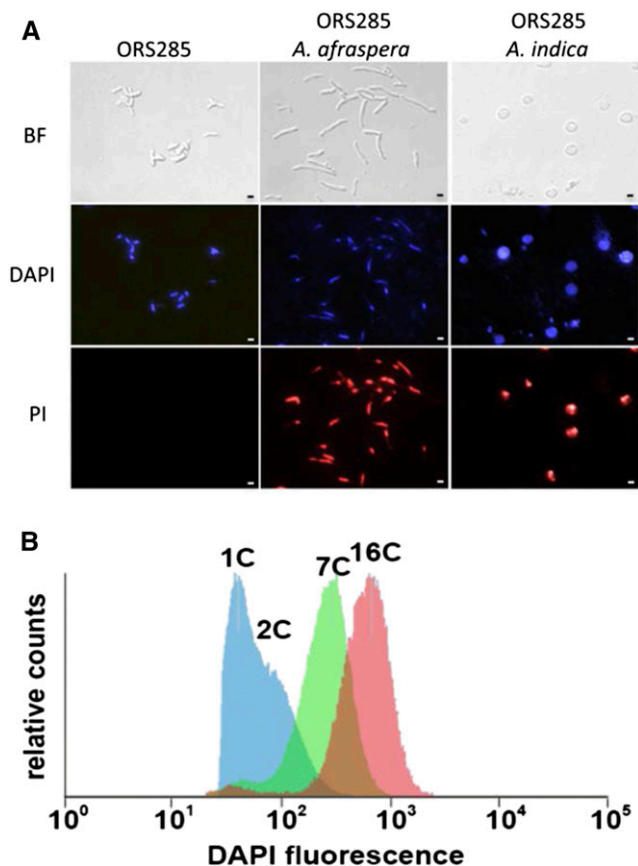
Figure 1. Properties of free-living cultured *Bradyrhizobium* sp. ORS285 bacteria and ORS285 bacteroids isolated from *A. afraspera* or *A. indica* nodules. A, Normaski bright-field (BF; top row) and fluorescence microcopy of bacteria and bacteroids stained with 4′,6-diamidino-2-phenylindole (DAPI; middle row) and PI (bottom row). Bars = 1 μm. B, DNA content of DAPI-stained bacteria and bacteroids measured by flow cytometry. Colors are as follows: blue, free-living bacteria; green, bacteroids isolated from *A. afraspera*; and red, bacteroids isolated from *A. indica*.

metamorphosis in *Medicago* spp., such as bacterial DNA content, membrane permeability, and viability. As revealed by flow cytometry analysis (Fig. 1B), the DNA content of E- and S-bacteroids peaked at around 7C and 16C, respectively, in comparison with the 1C/2C DNA content of free-living bacteria. These ploidy levels are less than described for *S. meliloti* bacteroids (24C; Mergaert et al., 2006), although other studies have shown lower ploidy levels also in *Medicago* spp. (Sinharoy et al., 2013; Berrabah et al., 2014).

Bacteroid membrane integrity was estimated using propidium iodide (PI), a DNA stain that is excluded from living cells but penetrates in cells displaying membrane integrity damage (Mergaert et al., 2006). Fluorescence images of the PI-stained bacteroids showed that the membrane permeability of E- and S-morphotype bacteroids was more prominent than that of the free-living bacteria (Fig. 1A). Indeed, 88% of S-bacteroids and 95% of E-bacteroids were found to be

permeable to PI against 7% for free-living bacteria. For comparison, PI stained about 50% of *S. meliloti* bacteroids (Mergaert et al., 2006). The loss of viability measured for S-morphotype bacteroids from *A. indica* nodules (98%) was also comparable to the one estimated previously for *S. meliloti* bacteroids (99%; Mergaert et al., 2006). In contrast, intracellular cells of *A. afraspera* appeared more viable, as 22% formed colonies on agar plates. However, this higher value could result from the fact that *A. afraspera* nodules displayed the unusual presence of two infected tissues, a large central tissue in which the bacteria are elongated and a superficial tissue in which the shape of the bacteria remained unmodified (Bonaldi et al., 2011). Therefore, the intracellular cells extracted from nodules consisted of a mixture of differentiated and nondifferentiated bacteria, suggesting that the loss of viability of E-morphotype bacteroids should be far more important. Taken together, we observed that the E- and S-morphotype bacteroids from *Aeschynomene* spp. nodules share the same features as the *S. meliloti* bacteroids in *Medicago* spp. and, therefore, that they can be considered as terminally differentiated.

Distribution of S- and E-Morphotype Bacteroids among *Aeschynomene* spp.

To obtain more insight into the distribution of the E- and S-bacteroid morphotypes among the *Aeschynomene* spp., we analyzed by confocal microscopy the shape of intracellular bacteria from mature nodules of various *Aeschynomene* spp. elicited by the ORS285 strain tagged with GFP. Unlike the other photosynthetic *Bradyrhizobium* spp. strains, such as ORS278 and BTAi1, this bacterium does contain the canonical *nodABC* genes and displays a broader host range due to its ability to use a Nod factor-dependent and a Nod factor-independent symbiotic process according to the host plant (Bonaldi et al., 2011). We observed in all tested species using a Nod factor-independent process (*A. indica*, *A. evenia* ssp. *serrulata*, *A. evenia.* ssp. *evenia*, *Aeschynomene virginica*, *Aeschynomene scabra*, and *Aeschynomene sensitiva*) that the bacteroids displayed an S-morphotype, whereas in the three Nod factor-dependent species tested (*A. afraspera*, *Aeschynomene nilotica*, and *Aeschynomene aspera*), the bacteroids displayed an E-morphotype (Fig. 2; Supplemental Fig. S1B).

We also analyzed the bacteroid shape in another group of *Aeschynomene* spp. not nodulated by the ORS285 strain but by nonphotosynthetic *Bradyrhizobium* spp. strains containing *nod* genes such as ORS301, ORS302, and ORS305 (Molouba et al., 1999). We also observed in these species (*Aeschynomene americana*, *Aeschynomene pfundii*, and *Aeschynomene schimperi*) that the bacteroids displayed an E-morphotype. Altogether, these data indicate that S-morphotype bacteroids are specific for the *Aeschynomene* spp. using a Nod factor-independent symbiotic process, while the E-morphotype is specific to the *Aeschynomene* spp. using a Nod factor-dependent one.
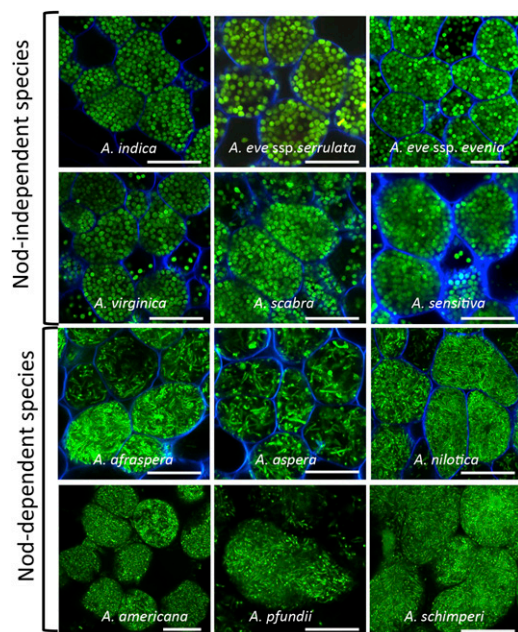
Figure 2. Distribution of S- and E-morphotype bacteroids among *Aeschynomene* ssp. The species *A. indica*, *A. evenia* ssp. *serrulata*, *A. evenia* spp. *evenia*, *A. virginica*, *A. scabra*, *A. sensitiva*, *A. afraspera*, *A. nilotica*, and *A. aspera* were nodulated by the ORS285 GFP-tagged strain; the species *A. americana*, *A. schimperi*, and *A. pfundii* were nodulated by *Bradyrhizobium* spp. strains ORS301, ORS302, and ORS305, respectively, and bacteroids were stained by the SYTO 9 fluorescent probe of the live/dead stain. Bars = 10 µm.

Aeschynomene spp. Contain a New Class of Nodule-Specific Cys-Rich Peptide-Encoding Genes

Our results indicate that in *Aeschynomene* spp. nodules, the endosymbiotic bacteria undergo terminal differentiation similar to that described in nodules of IRLC species. This raises the question of whether NCR peptides are also recruited in *Aeschynomene* spp. to govern this differentiation step. To check this possibility, we analyzed four EST libraries previously constructed in our laboratory and corresponding to noninoculated roots and mature nodules from *A. afraspera* and *A. indica* plants inoculated with the ORS285 strain. Although the total number of complementary DNAs (cDNAs) sequenced for each library was relatively small, around 9,500 ESTs per library (Supplemental Table S1), we postulated that if NCR peptides were also involved in bacteroid differentiation in *Aeschynomene* spp., they should be specifically and highly expressed in the nodules and, hence, easily detectable. We first performed a BLAST search on the EST libraries using several *M. truncatula* NCR genes as a query, but no conclusive results were obtained. Considering that NCR genes are rapidly evolving and are highly diverse, even within *M. truncatula* (Alunni et al., 2007; Branca et al., 2011), we reanalyzed the available EST databases using the following parameters determined from typical features of the NCR family: (1) candidate genes should

encode small proteins (less than 100 amino acids) containing a signal peptide; (2) the gene expression should be nodule specific with a significant read count in the EST database (we arbitrarily fixed a lower limit of five reads); and (3) the candidate genes should encode peptides rich in Cys residues (at least four). This second in silico analysis identified 15 genes encoding putative NCR-like peptides from the *A. afraspera* nodule library and 18 from the library of *A. indica* nodules (Fig. 3).

These genes were named *AaNCRs* or *AiNCRs* and numbered according to their rank in read counts (Supplemental Table S2). The deduced mature peptides (i.e. without their signal peptides) are between 37 and 85 residues long and contain four to 10 Cys residues (Fig. 3A). The alignment of these NCR-like peptides highlighted, for 31 out of the 33 sequences, a conserved pattern of six Cys residues within the sequence of the mature peptides (Fig. 3B). This pattern is very close to the one described previously for a group of *Medicago* spp. NCR peptides but distinct by the spacing between the first three Cys residues. This led us to propose a specific *Aeschynomene* spp. NCR-like motif. Interestingly, 11 of these NCR-like peptides contained two extra Cys residues, giving rise to a typical defensin signature that was named motif 2 (Fig. 3B).

By analogy with *M. truncatula*, for which the NCR family is composed of about 600 genes that exhibit distinct temporal and spatial expression patterns in nodules (Mergaert et al., 2006; Alunni et al., 2007; Young et al., 2011; Guefrachi et al., 2014), the involvement of a larger number of NCR genes is also expected in *Aeschynomene* spp. Therefore, we considered the possibility that our criteria were too selective, leading to a restricted number of candidate genes identified. By performing BLAST searches against the same EST libraries but this time using the first candidate genes that emerged, we identified a total of 38 and 44 NCR-like genes in *A. afraspera* and *A. indica*, respectively (Supplemental Table S2). All these additional genes were found to be specifically expressed in the nodules, and a global alignment shows that all of them except three contained the *Aeschynomene* spp. NCR-like motif 1 or 2.

Furthermore, a BLAST search against transcriptome data obtained from *A. evenia* ssp. *serrulata* mature nodules made by the 454 technology, which allows the detection of a larger number of transcripts, revealed an even higher number of NCR-like genes of more than 80 (Supplemental Table S2). Altogether, these data suggest that the NCR-like genes constitute also in *Aeschynomene* spp. an important family that could count several tens or even hundreds of members.

NCR-Like Genes of *Aeschynomene* spp. Are Expressed before or Concomitant with Bacteroid Differentiation

In order to analyze the temporal expression of the *AaNCR* and *AiNCR* genes, we performed a reverse transcription-quantitative PCR (RT-qPCR) analysis of four of them for each *Aeschynomene* spp. Root tissues of *A. afraspera* and *A. indica* were sampled at time 0 and at
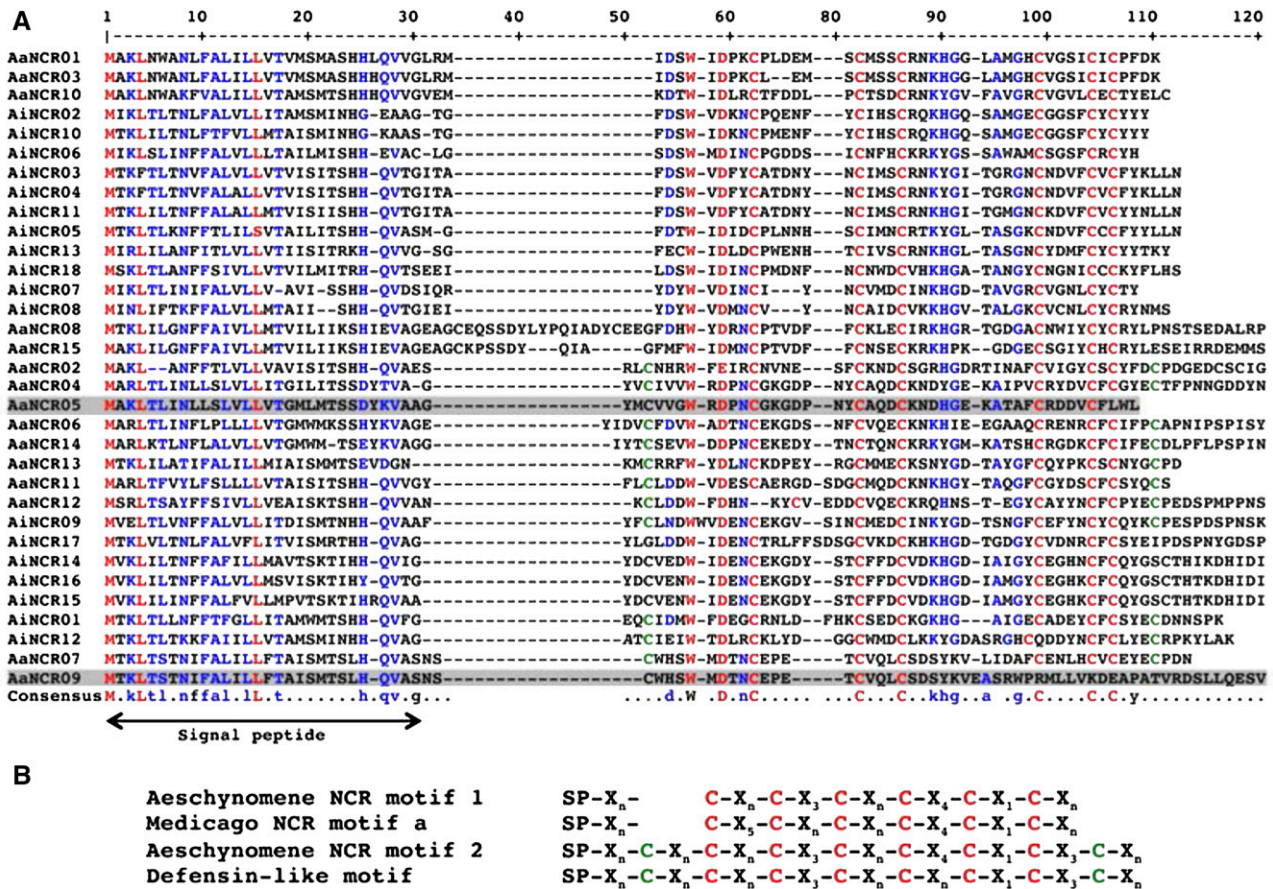
Figure 3. Alignment and Cys signature of *Aeschynomene* spp. NCR peptides. A, The deduced protein sequences from the up-regulated NCR genes from *A. indica* (AiNCRs) or *A. afraspera* (AaNCRs) were aligned using Multalin (http://multalin.toulouse. inra.fr/multalin/), and the alignment obtained was adjusted manually. Highly conserved amino acids are in red, and conservative substitutions are in blue. The putative location of the signal peptide is indicated below the alignment. B, Comparison of the Cys-rich motifs of *Aeschynomene* spp. NCR peptides with those of *Medicago* spp. and defensin-like peptides. Red and green Cys residues correspond to the NCR and defensin signatures, respectively. The peptides that do not contain any motif are gray shaded in A.

different time points after inoculation with *Bradyrhizobium* sp. strain ORS285 (6 h and 1, 2, 3, 4, 5, 6, 7, and 14 d). As a symbiotic marker, we also monitored *Leghemoglobin* (*LegHb*) mRNA accumulation. As shown in Figure 4, mRNA corresponding to *LegHb* started to accumulate at 5 dpi for both species (i.e. when the bacteroid differentiation process is completed and a nitrogenase activity is detectable; Bonaldi et al., 2011). Interestingly, while the NCR-like gene transcripts were not detected in control roots or during the early time points of nodule formation, they were all strongly expressed at 5 dpi, and some of them even started to accumulate 1 or 2 d before (Fig. 4), which coincided with the beginning of bacteroid morphogenesis (Bonaldi et al., 2011).

To complete this expression analysis, we also checked the expression by RT-qPCR, in both roots and nodules, of three candidate NCR genes identified in *A. evenia* by BLAST. As expected, the three genes appeared specifically and highly expressed in *A. evenia* nodules (Supplemental Fig. S2).

NCR-Like Genes Are Expressed Specifically in Infected Cells of *Aeschynomene* spp. Nodules

In *Medicago* spp., the NCR peptides are specifically synthesized in the infected plant cells and are targeted to the bacteria (Van de Velde et al., 2010). To check if the expression of the identified *AaNCR* and *AiNCR* genes was also restricted to the infected cells, we performed an in situ hybridization on 14-d-old nodules of *A. afraspera* and *A. indica* infected with the ORS285 strain. We used as probes *AaNCR01* and *AiNCR01*, which were found to be the most highly expressed *NCR* genes in each species. In addition, the *LegHb* gene, known to be expressed in infected nodule cells, was included as a positive control for the hybridization experiment. As shown in Figure 5, a strong signal was obtained using the *LegHb* antisense DNA as a probe. The signal was restricted to the infected cells (Fig. 5, B and E), consistent with the known role of this protein in symbiosis. Both *A. afraspera* and *A. indica NCR* antisense probes
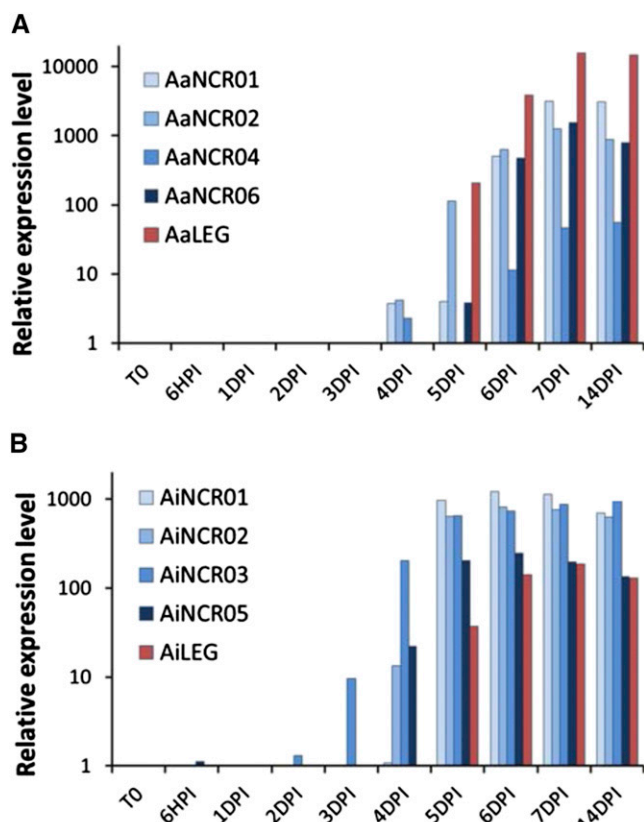
Figure 4. NCR expression during the symbiotic process. NCR expression is shown during *A. afraspera* (A) and *A. indica* (B) nodule development. Plants were inoculated with the *Bradyrhizobium* sp. ORS285 strain, and the roots were sampled at time 0 (T0) and at different time points as indicated. The relative expression level of the NCR peptides was determined by RT-qPCR and normalized by the expression of Elongation Factor 1α (EF1α). As a control of nodule development, the expression of *LegHb* (LEG) was also measured.

also gave a signal limited to the infected cells (Fig. 5, C and F), similar to what was observed for *LegHb*. Control hybridizations without probe or with a sense *LegHb* probe or sense *NCR-like* probes (Fig. 5, A and D) showed a complete absence of signal.

NCR-Like Peptides Target Bacteroids in *Aeschynomene* spp. Nodules

To test the possibility that AaNCR and AiNCR mature peptides are targeted to the endosymbiotic bacteria, we set up a proteome approach. Total protein extracts were prepared from nodules and from purified bacteroids from both *A. afraspera* and *A. indica*. In addition, a control extract was prepared from free-living ORS285 bacteria. Proteins were subjected to Tricine-PAGE analysis. Slight differences in the patterns of low-molecular-mass proteins (between 4 and 9 kD), where we expected the AaNCR or AiNCR peptides, could be observed between nodule or bacteroid extracts and extracts from free-living bacteria (Supplemental Fig. S3). We identified the

corresponding proteins by mass spectrometry. From the bacteroid extracts isolated from *A. afraspera* and *A. indica* nodules, 51 and 42 proteins were identified, respectively (Supplemental Table S3). Among them, in both nodule contexts, four corresponded to plant proteins, of which three were identified as NCR peptides (Table I). The additional plant protein identified in *A. indica* bacteroids was a putative monosaccharide-proton symporter corresponding probably to a symbiosome-located transporter, whereas there was an extensin-like protein of unknown function in *A. afraspera* bacteroids. Among the 40 proteins identified in free-living bacterial cells, all corresponded to bacterial proteins and none displayed the characteristics of Cys-rich peptides (Supplemental Table S3).

The DNF1 SPC Is Recruited for Bacteroid Differentiation in *Aeschynomene* spp.

To further support the role of the *Aeschynomene* spp. NCR peptides in bacterial differentiation, we applied a strategy aiming to interfere with their targeting to the symbiosomes, similar to that described before in *M. truncatula* (Van de Velde et al., 2010; Wang et al., 2010). NCR peptides are secretory proteins with an N-terminal signal peptide. Therefore, their transport requires the removal of this signal peptide by the SPC machinery, which is located in the membrane of the endoplasmic reticulum. Reduced SPC activity is supposed to hamper the transport of the NCR peptides to the symbiosomes, similar to that in the *dnf1* mutant of *M. truncatula* (Van de Velde et al., 2010; Wang et al., 2010).

To develop such a loss-of-function strategy in *Aeschynomene* spp., we chose to conduct this experiment on *A. evenia* ssp. *serrulata*, which is diploid, contrary to *A. indica* and *A. afraspera*, which are allopolyploids (Renard et al., 1983; Arrighi et al., 2014). A BLAST search using MtDNF1 allowed the identification in the *A. evenia* ssp. *serrulata* transcriptome database of a single candidate gene, which we named *AeDNF1*, encoding a protein of 167 amino acids with 83% identity (Fig. 6A). We used an RNA interference (RNAi) approach to knock down *AeDNF1*. The morphology of the bacteroids was observed in mature nodules elicited by the GFP-tagged ORS285 strain. In parallel, we monitored the level of *AeDNF1* extinction by RT-qPCR. As shown in Figure 6B, in transgenic lines in which the expression level of *AeDNF1* was not affected, the bacteroid differentiation occurred normally, giving rise to spherical bacteroids, while in the lines with the highest extinction level (about 65% reduction of *AeDNF1* expression), defects in bacteroid differentiation were observed with the presence of various bacteroid morphotypes within the same cell (Fig. 6C) or elongated bacteroids instead of spherical ones (Fig. 6, D and E).

DISCUSSION

The use of Cys-rich peptides called NCR peptides to govern bacteroid differentiation was assumed to be specific to legume species belonging to the IRLC clade,

Figure 5. NCR genes are specifically expressed in the infected symbiotic cells of *Aeschynomene* spp. nodules. Sections of 14-dpi *A. indica* and *A. afraspera* nodules, infected with the *Bradyrhizobium* sp. ORS285 strain, were analyzed by in situ hybridization with antisense probes of LegHb (B and E) or NCR (C and F). Control hybridizations were done with the sense NCR probe (A and D). Bars = 100 μm.
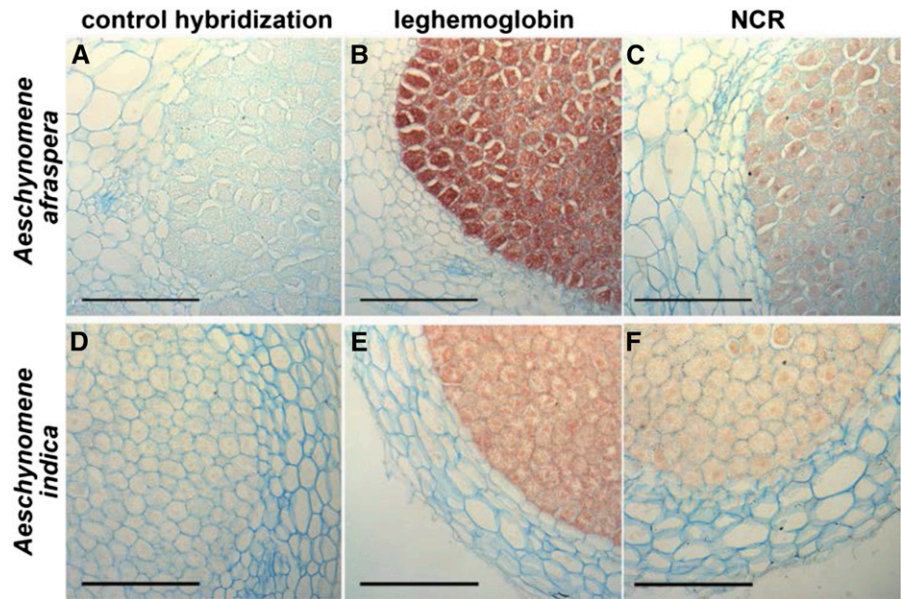
no homologs of NCR peptides being found in legume species outside of this clade (Mergaert et al., 2003). However, our data lead us to propose here that *Aeschynomene* spp. use a similar molecular mechanism to impose a differentiation process on their rhizobium endosymbionts.

First, we demonstrated that the distinguishing characters associated with bacteroid differentiation in nodules of IRLC legumes (i.e. marked cell enlargement, polyploidy, membrane permeability modification, and loss of viability) are conserved in *Aeschynomene* spp. nodules. Second, we identified in several *Aeschynomene* spp. a class of Cys-rich peptides that have similar characteristics to the *Medicago* spp. NCR peptides and that are synthesized specifically in nodule symbiotic cells and targeted to the bacteroids. Finally, silencing of the *dnf1* homolog in *A. evenia* ssp. *serrulata* impaired bacteroid differentiation. Moreover, it has been shown that *Bradyrhizobium* sp. strains ORS278 and ORS285 require the Bacteroid development A-like (BclA) peptide transporter for both E- and S-morphotype bacteroid differentiation in *Aeschynomene* spp. (Guefrachi et al., 2015). BclA is similar to *S. meliloti* Bacteroid development A (BacA), which is needed for bacteroid differentiation in *Medicago* spp. and which imports NCR peptides into the bacterial cells. BclA can functionally replace BacA for symbiosis and for peptide transport. Together, these observations suggest that, in *Aeschynomene* spp., E- or S-morphotype bacteroid differentiation is under the control of the NCR peptide family that we identified here.

These findings might be surprising, considering that, according to the *Aeschynomene* spp., the bacteroids display two distinct morphotypes (S- and E-morphotypes). This difference of morphological shape suggests distinct mechanisms governing bacterial morphogenesis. The change from a rod to a spherical shape as observed in *A. indica* and *A. evenia* during bacteroid differentiation resembles bacterial morphologies resulting from mutations that affect peptidoglycan synthesis and that were described in *Escherichia coli* (Young, 2003). Similarly, it has been shown in *Vibrio* spp. that some noncanonical D-amino acids could lead to a rod-to-sphere shape transition both via their incorporation into the peptidoglycan polymer and by regulating enzymes that synthesize and modify it (Lam et al., 2009). Therefore, the bacteroid morphology in *A. indica* or *A. evenia* is possibly associated with changes in the peptidoglycan cell wall architecture. This raises the question of whether the morphogenesis to the S-morphotype is governed by a specific class of NCR peptides targeting enzymes or genes involved in peptidoglycan synthesis or if additional plant effectors of a different nature such as particular D-amino acids are involved in the control of bacteroid morphogenesis.

Even if the underlying mechanisms for E- and S-morphotype bacteroid formation are obviously different, some observations strongly suggest that the two processes are closely related. In *A. indica* and *A. evenia*, the formation of the spherical bacteroids is taking place synchronously in all nodule cells between 4 and 5 dpi (Bonaldi et al., 2011). In this 1-d time frame, all intracellular rod-shaped bacteria transform into spheres. However, when making observations between 4 and 5 dpi, one can discern intermediate differentiation stages that strongly resemble E-morphotype bacteroids (Supplemental Fig. S4). In addition, we observed in the *A. evenia* ssp. *serrulata* knockdown lines, in which the level of expression of *AeDNF1* was reduced, bacteroids with an E-morphotype instead of an S-morphotype or a mixture of both shapes within the same cell. Finally, the bacterial gene *bclA* is similarly required for

Table I. *Mass spectrometry identification of proteins of plant origin from bacteroids isolated from A. afraspera and A. indica mature nodules*

This table is a compilation of all the plant proteins identified from bacteroid samples and processed by Mascot Distiller (version 2.1.1.0) software (Matrix Science).

Gene Name	Protein Function	Protein Mass	Mascot Protein Score	Protein Coverage	Peptide Sequences (5'–3')
		D		%	
Bacteroid *A. afraspera*-ORS285					
AaNCR15	NCR like	4,928	74	32.5	GDGECSGIYCHCR
AaNCR01	NCR like	8,714	56	16.9	CPLDEMSCMSSCR
AaNCR07	NCR like	7,928	53	31.3	VLIDAFCENLHCVCEYECPDN
AaCL26Contig2	Extensin-like protein	3,497	56	46.9	NIPISLSLILNVCSR
Bacteroid *A. indica*-ORS285					
ADL0ADA10YJ01CM1	Putative monosaccharide H⁺ symporter	20,215	52	4.3	LASSILPR
AiNCR02	NCR like	8,521	78	25.7	HGQSAMGECGGSFCYCYYY
			52	24.3	HGQSAMGECGGSFCYCYY
AiNCR18	NCR like	9,165	64	21.8	HGATANGYCNGNICCCK
AiNCR06	NCR like	8,471	124	52.1	YGSSAWAMCSGSFCR
					LGSDSWMDINCPGDDSICNFHCK

E-morphotype bacteroid formation in *A. afraspera* or S-morphotype bacteroid formation in *A. indica* or *A. evenia* (Guefrachi et al., 2015).

Interestingly, analysis of the distribution of the E- and S-morphotype bacteroids among *Aeschynomene* revealed that all the tested species using a Nod factor-independent symbiotic process have S-morphotype bacteroids, whereas those using a Nod factor-dependent process have E-morphotype bacteroids, similar to the IRLC species. Furthermore, a recent phylogenetic analysis revealed that all *Aeschynomene* spp. using a Nod factor-independent symbiotic process form a monophyletic clade that does not include other species using a Nod factor-dependent process (Supplemental Fig. S1B; Chaintreuil et al., 2013). Therefore, it would be tempting to speculate that the S-morphotype of bacteroids and Nod factor-independent symbiosis are both derived characters, which are correlated. However, in the Dalbergioid clade that contains the *Aeschynomene* genus, other species, such as *A. hypogaea* or *Stylosanthes hanata*, also host spherical bacteroids (Chandler et al., 1982). It has been established that at least *A. hypogaea* uses a Nod factor-dependent symbiotic process (Ibáñez and Fabra, 2011). This suggests that the S-morphotype character emerged several times during the diversification of the Dalbergioid clade independently from the Nod factor-independent character.

The mode of action of the NCR peptides and their bacterial targets remains unclear in *Medicago* spp. However, it has been shown that some cationic NCR peptides are able to provoke symptoms of terminal differentiation in vitro (Van de Velde et al., 2010). To examine if the NCR peptides identified in *Aeschynomene* spp. could induce the same symptoms in vitro, we tested the activity of five synthetic *Aeschynomene* spp. NCR peptides (AaNCR01, AaNCR02, AiNCR01, AiNCR02, and AiNCR03), which are the most abundant ones identified in the *A. afraspera* and *A. indica*

nodule EST libraries. No activity could be detected on *Bradyrhizobium* sp. strain ORS285 (Supplemental Fig. S5A). Nevertheless, one of them (AaNCR01) displayed a weak antimicrobial activity on *S. meliloti* and could provoke a slight increase in the bacterial ploidy level (Supplemental Fig. S5, B and C). We also tested on the strain ORS285 the *Medicago* spp. NCR peptides (NCR035, NCR247, and NCR335) known to have an antimicrobial effect on a large panel of bacteria (Tiricz et al., 2013), but surprisingly, no activity was detected for those peptides, whereas on the control *S. meliloti* strain, strong antimicrobial activity and membrane damage could be observed under the same conditions. The membrane of *Bradyrhizobium* spp. strains differs from that of rhizobium strains by the presence of hopanoids, which may represent up to 40% of the total lipid extract (Kannenberg et al., 1995). It was recently shown that this class of compounds, which display some structural similarity with eukaryotic sterols, reinforce the stability and rigidity of the outer membrane of photosynthetic *Bradyrhizobium* spp. (Silipo et al., 2014). It is possible, therefore, that hopanoids reduce the antimicrobial activity of cationic *Medicago* NCR peptides by reinforcing the outer membrane barrier function. In agreement with this assumption, we observed that a hopanoid mutant of the photosynthetic *Bradyrhizobium* spp. strain BTAi1 was highly sensitive to the *Medicago* NCR peptides, in contrast to the wild-type strain (Supplemental Fig. S5A). Nevertheless, this mutant still remained resistant to the *Aeschynomene* spp. NCR peptides tested (Supplemental Fig. S5A).

The lack of activity of the tested *Aeschynomene* NCR peptides in vitro on the ORS285 strain or on the BTAi1 hopanoid mutant could result from the fact that they have a net neutral or negative charge. Indeed, in *Medicago* spp., only cationic NCR peptides, particularly those with a high pI, were reported so far to display in vitro activity. This does not imply that anionic or neutral NCR peptides are not functional in vivo,

Figure 6. *DNF1* silencing affects bacteroid differentiation in *Aeschynomene* spp. A, Alignment of the deduced protein sequence of the *A. evenia* ssp. *serrulata DNF1* ortholog with the corresponding *Medicago* spp. protein (accession no. TC121074). The two protein sequences were aligned using Multalin (http://multalin.toulouse.inra.fr/multalin/). B to E, Roots of different lines of *A. evenia* ssp. *serrulata* transformed with an RNAi construct directed against *AeDNF1* encoding the SPC22 subunit of the SPC were inoculated with a GFP-tagged *Bradyrhizobium* sp. ORS285 strain. At 21 dpi, the nodules were harvested, and the shape of the bacteroids was observed by confocal microscopy on nodule sections. As a control, a line with no RNAi effect (1% reduction) was used (B). The lines 3, 7, and 53, with expression levels reduced by 62%, 65%, and 66%, respectively, are presented in C to E. Bars = 10 μm.
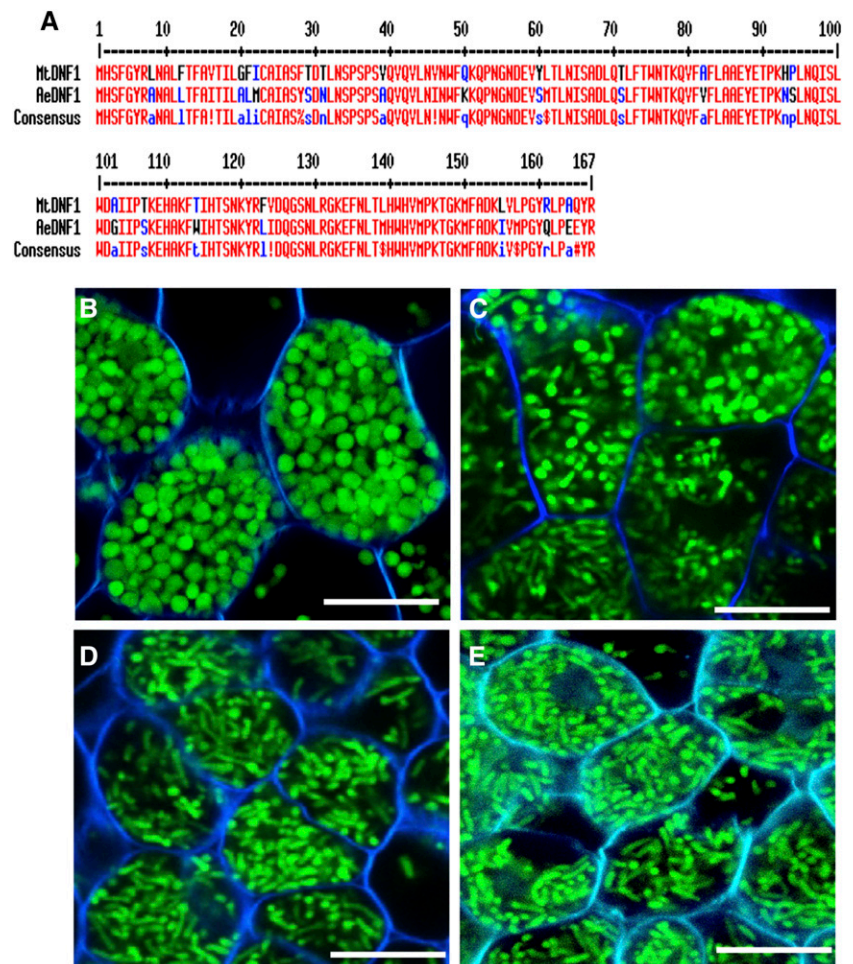
considering their high level of expression, which is similar to that of the cationic NCR peptides (Mergaert et al., 2003). It was proposed that the cationic NCR peptides interact preferentially with the negatively charged outer membrane of rhizobia and, by compromising its permeability, facilitate the entry of anionic NCR peptides to the bacterial cytosol (Kondorosi et al., 2013). In *Aeschynomene* spp., except for two *A. indica* NCR peptides with a pI close to 8, no cationic NCR-like peptides could be identified among the several tens of candidate genes identified in each species (Supplemental Table S2). However, we cannot exclude that such a class of cationic NCR peptides does exist in *Aeschynomene* spp. Our transcriptomic analyses made on mature nodules at 14 dpi could have missed these NCR peptides that are more likely to act earlier in the differentiation process. Furthermore, the difference in the membrane ultrastructure between bradyrhizobia and rhizobia could also imply a mechanism other than electrostatic binding and a specific class of NCR peptides that we have not yet identified. The understanding of how *Aeschynomene* spp. NCR peptides can enter in *Bradyrhizobium* spp. cells and modulate their physiology and morphology will require further studies.

In silico analyses of the available transcriptome databases suggest the NCR-like genes constitute an important family in *Aeschynomene* spp. that could count several tens or even hundreds of candidates. As observed for *Medicago* spp., the amino acid sequences of these NCR peptides are highly divergent except for the distribution of six Cys residues, which is conserved in more than 90% of the identified peptides. A phylogenetic analysis based on the sequences of the mature peptides shows that the NCR-like peptides identified in *Aeschynomene* spp. are distant from the NCR peptides identified in IRLC (Supplemental Fig. S6). A recent study mapping the bacteroid morphology in 40 legume species of the Papilionoideae suggests that legumes inducing bacteroid morphogenesis evolved independently at least five times from an ancestral papilionoid legume hosting U-morphotype bacteroids (Oono et al., 2010). It has been proposed that the NCR family identified in IRLC legumes evolved from defensin ancestors (Mergaert et al., 2003). This large family of antimicrobial peptides is found in all eukaryotes, where they are part of the first line of defense against invading microbes. The fact that the NCR peptides identified in *Aeschynomene* spp. are phylogenetically distant from

the NCR peptides identified in the IRLC legumes but also display a defensin signature suggest that they have similarly evolved from defensins but likely from a distinct ancestral repertoire.

It will be interesting to determine if the use of Cys-rich peptides is a general strategy in legumes to keep their endosymbionts under control and to analyze the transcriptomes of nodules from species belonging to the two other lineages, the genistoids and the mirbelioids, in which bacteroid morphogenesis was reported, using the selective criteria defined in this study. Remarkably, it was shown recently that also actinorhizal plants forming nodules with bacteria from the *Frankia* genus (Carro et al., 2015), as well as insects, produce symbiosis-specific antimicrobial peptides to control the development of their endosymbiotic bacteria, which display in certain cases a spherical or elongated shape similar to the S- or E-morphotype bacteroids (Login et al., 2011; Shigenobu and Stern, 2013). This suggests that the enrollment of antimicrobial peptides as symbiosis effectors is an optimal modus operandi for a eukaryotic host cell to control large populations of intracellular bacteria.

MATERIALS AND METHODS

Bacterial Strains and Growth Conditions

Bradyrhizobium spp. strain ORS285 tagged or not with GFP (Bonaldi et al., 2011) and *Bradyrhizobium* spp. strains ORS301, ORS302, and ORS305 (Molouba et al., 1999) were grown at 37°C in yeast mannitol medium (Vincent, 1970). The medium used for ORS285::GFP was supplemented with kanamycin (50 μg mL^{-1}).

Plant Material, Growth Conditions, and Inoculation

All the accessions of *Aeschynomene* spp. used in this study, their geographic origins, their sources, and the *Bradyrhizobium* spp. strains used to inoculate them are listed in Supplemental Table S4. Seed germination, plant culture, and bacterial inoculation were performed as before (Bonaldi et al., 2011).

Bacteroid Characterization

Bacteroid isolation was performed as described (Mergaert et al., 2006). Bacteroids and free-living bacteria were stained with DAPI at 50 μg mL^{-1} and PI at 2 μg mL^{-1} and observed with a Reichert Polyvar fluorescence microscope equipped with a Nikon dxm 1200 digital camera. DNA measurements were performed with a Beckman-Coulter ELITE ESP flow cytometer. For counting of cultivable bacterial cells, bacteroid suspensions were serially diluted in 10-fold dilutions and plated on yeast mannitol agar plates. At the same time, the cells in the bacteroid suspensions were also directly counted by light microscopy using a Malassez cell-counting chamber.

Analysis of the Bacteroid Morphotype in Various *Aeschynomene* spp.

Semithin nodule sections (30 to 40 μm thick) were prepared using a Vibratome (VT1000S; Leica). Nodules elicited by the ORS285-tagged GFP strain were visualized as described previously (Bonaldi et al., 2011). For the nodules elicited with the nontagged strains, the nodule sections were incubated for 15 min in live/dead staining solution (5 μM SYTO 9 and 30 μM PI in 50 mM Tris, pH 7 buffer; Live/Dead BacLight; Invitrogen). Sections were then removed and incubated an additional 15 min in 10 mM phosphate saline buffer containing Calcofluor White M2R (Sigma) to a final concentration of 0.01% (w/v) to stain the plant cell wall (Nagata and Takebe, 1970). Analyses were carried out using a confocal laser-scanning microscope (Carl Zeiss LSM 700). Calcofluor White was excited at 405 nm with emission signal collection at 405 to 470 nm. For SYTO 9 and PI, excitation wavelengths of 488 and 555 nm were used with emission signal collection at 490 to 522 nm and 555 to 700 nm, respectively. Images were obtained using the ZEN 2008 software (Zeiss).

EST Libraries

For the *Aeschynomene afraspera* and *Aeschynomene indica* EST libraries, total RNA was extracted from uninoculated roots and from mature nodules (14 dpi with *Bradyrhizobium* spp. strain ORS285) using the RNeasy plant mini kit (Qiagen). The root and nodule EST libraries were constructed using the Creator Smart cDNA Library kit (Clontech). For each library, 15,000 clones were randomly processed through the Genoscope genomic and robotic platform for single-read sequencing from the 5' end (www.genoscope.cns.fr). For *A. afraspera*, 9,492 and 9,582 sequences were obtained from roots and nodules, respectively, and 9,621 and 9,847 sequences were obtained for *A. indica* (http://esttik.cirad.fr).

In Situ Hybridization

A. indica and *A. afraspera* nodules were harvested at 14 dpi and fixed immediately with 4% (w/v) paraformaldehyde containing 0.1% (w/v) Tween 20 and 0.1% (w/v) Triton X-100 at 4°C overnight. Nodule tissues were dehydrated by incubation in increasing concentrations of ice-cold ethanol series. They were then embedded in paraffin blocks (Javelle et al., 2011). Sections (7 μm thick) were cut with a microtome (RM2155; Leica). Sections were adhered on poly-L-Lys-coated slides, and paraffin was subsequently removed with Histoclear and Histoclear/ethanol series.

To produce the hybridization probes, PCR products of approximately 200 bp of the genes of interest were cloned into the pGEM-T Easy plasmid. The inserts were then amplified by PCR using the vector-specific T7 and SP6 primers flanking the insert. These primers correspond to the bacteriophage SP6 and T7 RNA polymerase promoters. RNA probes, labeled with digoxigenin, were obtained by in vitro transcription using the PCR product as a template and the T7 RNA polymerase of the DIG RNA labeling kit (SP6/T7; Roche). Antisense probes were used to detect the location of transcripts of interest, and sense probes were used as negative controls. A control without probe was also performed. Prehybridization, hybridization, and posthybridization treatments and mounting were done by a method derived from the procedure described by Javelle et al. (2011). To reveal the hybridization signal, an anti-digoxigenin antibody coupled to alkaline phosphatase was used with its substrate, 4-nitroblue tetrazolium chloride/5-bromo-4-chloro-3-indolyl-phosphate, which forms a brownish precipitate. The slides were finally observed with a Reichert Polyvar epifluorescence microscope combined with a Retiga 2000 CCD camera (QImaging).

Proteome Analysis

Crude protein extracts of nodules, bacteroids, and cultured *Bradyrhizobium* sp. ORS285 were half-diluted with Novex Tricine SDS sample buffer (2×). These samples were reduced (5 mM tributylphosphine, 30 min at 60°C) and alkylated (50 mM iodoacetamide, 30 min in the dark at room temperature) before the analyses by Novex 10% to 20% (w/v) Tricine Protein Gels (Life Technologies). Proteins in the range of approximately 4 to 9 kD (indicated with the dashed line in Supplemental Fig. S3) from free-living bacteria and bacteroid extracts were cut out from Tricine SDS-PAGE gels and identified by liquid chromatography-tandem mass spectrometry analysis (for detailed procedure, see Supplemental Text S1).

DNF1 Silencing

The *A. evenia* ssp. *serrulata DNF1* homolog was identified from the transcriptome reference library. A BLAST search using the *Medicago* spp. signal peptidase protein sequence allowed the identification of a single candidate, CL5310_contig1. This cluster of 1,041 bp encodes a protein of 167 amino acids with 83% identity with MtDNF1 and was named *AeDNF1* (Fig. 6A). For the RNAi strategy, a 283-bp internal fragment located between positions 16 to 298 of the *AeDNF1* cDNA cluster sequence was PCR amplified from root cDNA using specific primers (Supplemental Table S5). After insertion into pENTR through TOPO cloning (Invitrogen), the fragment was introduced into the binary pK7GWIWG2_II-RedRoot vector (Plant Genetic System) by Gateway technology to generate the hairpin construct. The construct was verified by PCR and DNA sequencing before introduction into the *Agrobacterium rhizogenes* ARqua1 strain for root transformation as described before (Arrighi et al., 2012). As a control, the same plasmid containing a GUS gene fragment was used. Transformed roots were selected by their red fluorescence under UV light resulting from the constitutive expression of the red fluorescent protein, and one root was conserved per plant. To assess the *AeDNF1* extinction level, quantitative reverse transcription-PCR was performed.

Real-Time Quantitative PCR Expression Analyses

Total RNA was extracted from roots or nodules at different time points after inoculation using the SV Total RNA Isolation System (Promega) and quantified using a NanoDrop ND-1000 spectrophotometer. Two hundred nanograms per sample was reverse transcribed using SuperScriptII reverse transcriptase (Invitrogen) and oligo(dT)$_{12–18}$ primers. Real-time quantitative PCR was performed by using the Brilliant II SYBR Green QPCR Master Mix (Agilent Technologies). The primers used for quantitative PCR are provided in Supplemental Table S5. The real-time SYBR Green cycling PCR program on a Stratagene MX3005P (Agilent Technologies) was as follows: one cycle at 95°C for 10 min; 40 cycles at 95°C for 10 s, 60°C for 30 s, and 72°C for 30 s; followed by one cycle at 95°C for 1 min, 55°C for 30 s, and 95°C for 30s. Reactions were performed in triplicate, and the efficiency-corrected comparative quantification method was used to quantify gene expression (Pfaffl, 2001). The results were standardized with $AeEF1\alpha$ expression levels.

Sequence data from this article can be found in the GenBank/EMBL data libraries under accession numbers FO981374 to FO99999 and LO000008 to LO016971.

Supplemental Data

The following supplemental materials are available.

Supplemental Figure S1. Distribution of bacteroid morphotypes among legumes.

Supplemental Figure S2. Nodule-specific expression of NCR genes in *A. evenia*.

Supplemental Figure S3. NCR peptides colocalize with bacteroids in *A. afraspera* and *A. indica* nodules.

Supplemental Figure S4. Change in the bacterial cell shape during the symbiotic interaction between *Bradyrhizobium* spp. strain ORS285 and *A. indica*.

Supplemental Figure S5. In vitro effect of synthetic *Aeschynomene* spp. and *Medicago* spp. NCR peptides.

Supplemental Figure S6. Neighbor-joining phylogeny of NCR protein sequences.

Supplemental Table S1. *A. afraspera* and *A. indica* root and nodule ESTs and cluster collection statistics.

Supplemental Table S2. Nodule-specific Cys-rich putative peptides from *A. indica*, *A. afraspera*, and *A. evenia*.

Supplemental Table S3. Protein identification by mass spectrometry in ORS285 free-living state and ORS285 bacteroids isolated from *A. indica* and *A. afraspera* nodules.

Supplemental Table S4. Accessions and origins of the *Aeschynomene* spp. used in this study.

Supplemental Table S5. Primer pairs used in this study and their utilization.

Supplemental Text S1. Supplemental materials and methods.

LITERATURE CITED

Alunni B, Kevei Z, Redondo-Nieto M, Kondorosi A, Mergaert P, Kondorosi E (2007) Genomic organization and evolutionary insights on GRP and NCR genes, two large nodule-specific gene families in *Medicago truncatula*. Mol Plant Microbe Interact **20:** 1138–1148

Arrighi JF, Cartieaux F, Brown SC, Rodier-Goud M, Boursot M, Fardoux J, Patrel D, Gully D, Fabre S, Chaintreuil C, et al (2012) *Aeschynomene evenia*, a model plant for studying the molecular genetics of the nod-independent rhizobium-legume symbiosis. Mol Plant Microbe Interact **25:** 851–861

Arrighi JF, Chaintreuil C, Cartieaux F, Cardi C, Rodier-Goud M, Brown SC, Boursot M, D'Hont A, Dreyfus B, Giraud E (2014) Radiation of the Nod-independent *Aeschynomene* relies on multiple allopolyploid speciation events. New Phytol **201:** 1457–1468

Berrabah F, Bourcy M, Eschstruth A, Cayrel A, Guefrachi I, Mergaert P, Wen J, Jean V, Mysore KS, Gourion B, et al (2014) A nonRD receptor-like kinase prevents nodule early senescence and defense-like reactions during symbiosis. New Phytol **203:** 1305–1314

Bonaldi K, Gargani D, Prin Y, Fardoux J, Gully D, Nouwen N, Goormachtig S, Giraud E (2011) Nodulation of *Aeschynomene afraspera* and *A. indica* by photosynthetic *Bradyrhizobium* sp. strain ORS285: the nod-dependent versus the nod-independent symbiotic interaction. Mol Plant Microbe Interact **24:** 1359–1371

Branca A, Paape TD, Zhou P, Briskine R, Farmer AD, Mudge J, Bharti AK, Woodward JE, May GD, Gentzbittel L, et al (2011) Whole-genome nucleotide diversity, recombination, and linkage disequilibrium in the model legume *Medicago truncatula*. Proc Natl Acad Sci USA **108:** E864–E870

Carro L, Pujic P, Alloisio N, Fournier P, Boubakri H, Hay AE, Poly F, François P, Hocher V, Mergaert P, et al (2015) *Alnus* peptides modify membrane porosity and induce the release of nitrogen-rich metabolites from nitrogen-fixing *Frankia*. ISME J **9:** 1723–1733

Chaintreuil C, Arrighi JF, Giraud E, Miché L, Moulin L, Dreyfus B, Munive-Hernández JA, Villegas-Hernandez MdelC, Béna G (2013) Evolution of symbiosis in the legume genus *Aeschynomene*. New Phytol **200:** 1247–1259

Chandler MR, Date RA, Roughley RJ (1982) Infection and root-nodule development in *Stylosanthes* species by *Rhizobium*. J Exp Bot **33:** 47–57

Giraud E, Hannibal L, Fardoux J, Verméglio A, Dreyfus B (2000) Effect of *Bradyrhizobium* photosynthesis on stem nodulation of *Aeschynomene sensitiva*. Proc Natl Acad Sci USA **97:** 14795–14800

Giraud E, Moulin L, Vallenet D, Barbe V, Cytryn E, Avarre JC, Jaubert M, Simon D, Cartieaux F, Prin Y, et al (2007) Legumes symbioses: absence of Nod genes in photosynthetic bradyrhizobia. Science **316:** 1307–1312

Guefrachi I, Nagymihaly M, Pislariu CI, Van de Velde W, Ratet P, Mars M, Udvardi MK, Kondorosi E, Mergaert P, Alunni B (2014) Extreme specificity of NCR gene expression in *Medicago truncatula*. BMC Genomics **15:** 712

Guefrachi I, Pierre O, Timchenko T, Alunni B, Barriere Q, Czernic P, Villaécija-Aguilar JA, Verly C, Bourge M, Fardoux J, et al (July 8, 2015) *Bradyrhizobium* BclA is a peptide transporter required for bacterial differentiation in symbiosis with *Aeschynomene* legumes. Mol Plant Microbe Interact http://dx.doi.org/10.1094/MPMI-04-15-0094-R

Haag AF, Arnold MF, Myka KK, Kerscher B, Dall'Angelo S, Zanda M, Mergaert P, Ferguson GP (2013) Molecular insights into bacteroid development during Rhizobium-legume symbiosis. FEMS Microbiol Rev **37:** 364–383

Ibáñez F, Fabra A (2011) Rhizobial Nod factors are required for cortical cell division in the nodule morphogenetic programme of the Aeschynomeneae legume Arachis. Plant Biol (Stuttg) **13:** 794–800

Javelle M, Marco CF, Timmermans M (2011) *In situ* hybridization for the precise localization of transcripts in plants. J Vis Exp **23:** e3328

Kannenberg EL, Perzl M, Härtner T (1995) The occurrence of hopanoid lipids in *Bradyrhizobium* bacteria. FEMS Microbiol Lett **127:** 255–262

Kondorosi E, Mergaert P, Kereszt A (2013) A paradigm for endosymbiotic life: cell differentiation of Rhizobium bacteria provoked by host plant factors. Annu Rev Microbiol **67:** 611–628

Lam H, Oh DC, Cava F, Takacs CN, Clardy J, de Pedro MA, Waldor MK (2009) D-Amino acids govern stationary phase cell wall remodeling in bacteria. Science **325:** 1552–1555

Login FH, Balmand S, Vallier A, Vincent-Monégat C, Vigneron A, Weiss-Gayet M, Rochat D, Heddi A (2011) Antimicrobial peptides keep insect endosymbionts under control. Science **334:** 362–365

Mergaert P, Nikovics K, Kelemen Z, Maunoury N, Vaubert D, Kondorosi A, Kondorosi E (2003) A novel family in *Medicago truncatula* consisting of more than 300 nodule-specific genes coding for small, secreted polypeptides with conserved cysteine motifs. Plant Physiol **132:** 161–173

Mergaert P, Uchiumi T, Alunni B, Evanno G, Cheron A, Catrice O, Mausset AE, Barloy-Hubler F, Galibert F, Kondorosi A, et al (2006) Eukaryotic control on bacterial cell cycle and differentiation in the Rhizobium-legume symbiosis. Proc Natl Acad Sci USA **103:** 5230–5235

Molouba F, Lorquin J, Willems A, Hoste B, Giraud E, Dreyfus B, Gillis M, de Lajudie P, Masson-Boivin C (1999) Photosynthetic bradyrhizobia from *Aeschynomene* spp. are specific to stem-nodulated species and form

a separate 16S ribosomal DNA restriction fragment length polymorphism group. Appl Environ Microbiol 65: 3084–3094

Nagata T, Takebe I (1970) Cell wall regeneration and cell division in isolated tobacco mesophyll protoplasts. Planta 92: 301–308

Oono R, Schmitt I, Sprent JI, Denison RF (2010) Multiple evolutionary origins of legume traits leading to extreme rhizobial differentiation. New Phytol 187: 508–520

Pfaffl MW (2001) A new mathematical model for relative quantification in real-time RT-PCR. Nucleic Acids Res 29: e45

Renard R, Lambinon J, Reekmans M, Van der Veken P, Govaert M (1983) Nombres chromosomiques de quelques Angiospermes du Rwanda, du Burundi et du Kenya. Bull Jard Bot Nat Belg 53: 342–371

Sen D, Weaver RW (1984) A basis for different rates of N2-fixation by the same strains of Rhizobium in peanut and cowpea root nodules. Plant Sci Lett 34: 239–246

Shigenobu S, Stern DL (2013) Aphids evolved novel secreted proteins for symbiosis with bacterial endosymbiont. Proc Biol Sci 280: 20121952

Silipo A, Vitiello G, Gully D, Sturiale L, Chaintreuil C, Fardoux J, Gargani D, Lee HI, Kulkarni G, Busset N, et al (2014) Covalently linked hopanoid-lipid A improves outer-membrane resistance of a *Bradyrhizobium* symbiont of legumes. Nat Commun 5: 5106

Sinharoy S, Torres-Jerez I, Bandyopadhyay K, Kereszt A, Pislariu CI, Nakashima J, Benedito VA, Kondorosi E, Udvardi MK (2013) The C_2H_2

transcription factor REGULATOR OF SYMBIOSOME DIFFERENTIATION represses transcription of the secretory pathway gene VAMP721a and promotes symbiosome development in *Medicago truncatula*. Plant Cell 25: 3584–3601

Tiricz H, Szucs A, Farkas A, Pap B, Lima RM, Maróti G, Kondorosi É, Kereszt A (2013) Antimicrobial nodule-specific cysteine-rich peptides induce membrane depolarization-associated changes in the transcriptome of Sinorhizobium meliloti. Appl Environ Microbiol 79: 6737–6746

Van de Velde W, Zehirov G, Szatmari A, Debreczeny M, Ishihara H, Kevei Z, Farkas A, Mikulass K, Nagy A, Tiricz H, et al (2010) Plant peptides govern terminal differentiation of bacteria in symbiosis. Science 327: 1122–1126

Vincent JM (1970) A Manual for the Practical Study of Root-Nodule Bacteria. Blackwell Scientific Publications, Oxford

Wang D, Griffitts J, Starker C, Fedorova E, Limpens E, Ivanov S, Bisseling T, Long S (2010) A nodule-specific protein secretory pathway required for nitrogen-fixing symbiosis. Science 327: 1126–1129

Young KD (2003) Bacterial shape. Mol Microbiol 49: 571–580

Young ND, Debellé F, Oldroyd GE, Geurts R, Cannon SB, Udvardi MK, Benedito VA, Mayer KF, Gouzy J, Schoof H, et al (2011) The *Medicago* genome provides insight into the evolution of rhizobial symbioses. Nature 480: 520–524